DOI: 10.48011/asba.v2i1.1484

Move blocking Model Predictive Control of a helicopter with three degrees of freedom ⋆

Rogério Toniere Giovanelli *,**
Rubens Junqueira Magalhães Afonso ***,****

* *Graduate Studies in Electronics and Computer Engineering – Systems and Control (PG/EEC-S), Instituto Tecnológico de Aeronáutica. Praça Marechal Eduardo Gomes, 50, 12228-900, São José dos Campos, SP, Brazil (e-mail: rogeriogiovanelli@outlook.com).*
** *Product Development Engineer – Control Laws, Embraer. Avenida Brigadeiro Faria Lima, 2170, 12227-901, São José dos Campos, SP, Brazil (e-mail: rogerio.giovanelli@embraer.net.br)*
*** *Institute of Flight System Dynamics, Technical University of Munich, Boltzmannstraße 15, 85748, Garching bei München, Germany (e-mail: rubens.afonso@tum.de).*
**** *Electronic Engineering Division, Instituto Tecnológico de Aeronáutica. Praça Marechal Eduardo Gomes, 50, 12228-900, São José dos Campos, SP, Brazil (e-mail: rubensjm@ita.br).*

Abstract: This work presents the use of a move blocking algorithm in the Model Predictive Control (MPC) of a helicopter with three degrees of freedom (3DoF). Considerations about the feasibility of the MPC solutions and robustness of the control law are developed to propose an internal feedback gain array using Linear Matrix Inequalities (LMIs). The objective of this structure is to grant adjustment flexibility of the plant dynamics through a $\mathfrak{D}$-stable region and to reduce the computational complexity of the problem.

Keywords: Model Predictive Control; move blocking; 3DoF helicopter; Linear Matrix Inequalities; $\mathfrak{D}$-stability.

1. INTRODUCTION

Model-based Predictive Control (MPC) computes control actions by the iterative solution of an optimization problem with a finite horizon using the current states of the system as the initial condition (Mayne et al., 2000). A control sequence is calculated at each sampling period, and its first elements are routed as commands to the respective actuator. Afterward, the feedback of the system output or state occurs, and the optimization problem is solved recursively from this condition. This policy is called Receding Horizon Control (RHC) (Maciejowski, 2002). The optimization object in question is a cost function that gives performance guidelines to the desired response of the system (Rossiter, 2003). Restrictions on the states and control signals can be considered, usually leading to numerical optimization problems. The performance and systematic modeling of this strategy are attractive for its application in the control of systems with multiple inputs and outputs, subjected to dynamically coupled states, constraints on the excursion of responses, and external disturbances.

The MPC efficiency is directly related to the accuracy level formulated to model the plant and the size of the prediction horizon adopted. However, these characteristics must be weighed against the computational capacity installed to accomplish the iterative feasibility of the solutions in real-time. Equivalently, the numerical complexity of this problem has the number of optimization variables as a dominant factor, given by the product of the m inputs of the system by the M control horizon steps. One way to handle this issue is to adopt a move blocking algorithm, which holds the input value or its derivatives constant for several sampling periods (Cagienard et al., 2007).

In the present work, predictive control with a move blocking strategy, as detailed in Cagienard et al. (2007), is explored. The object of study is the linear model of an educational 3DoF helicopter from manufacturer Quanser Consulting, which is installed at the Computer Control Laboratory of the Electronic Engineering Division of the Instituto Tecnológico de Aeronáutica. The control architecture proposed by Cagienard et al. (2007) is based on an algorithm to generate move blocking matrices that shift blocked control inputs at each iteration of the MPC. Additionally, there is an internal control-loop with static gains calculated via an algebraic Riccati equation to guarantee stability and recursive feasibility to the final system. Previous studies developed around the 3DoF helicopter addressed the use of MPC strategy variations to deal with plant modeling uncertainty characteristics and processing time (Caregnato Neto, 2018; Chung, 2017; Pascoal, 2010).

⋆ Rubens Afonso acknowledges the support of CAPES (fellowship proc. #88881.145490/2017-01) and the Federal Ministry for Education and Research of Germany through the Alexander von Humboldt Foundation.

The contribution in the present paper involves computing the internal control-loop gains through Linear Matrix Inequalities (LMIs) to change the dynamics of the plant respecting a $\mathfrak{D}$-stable region, maintaining the recursive feasibility and asymptotic stability properties demonstrated in Cagienard et al. (2007).

Therefore, the contributions brought by the present work include a demonstration that the proposed LMIs to compute the gains of the internal closed-loop satisfy the stability and recursive feasibility of the predictive control (external closed-loop). An advantage of using LMIs is the ability to add $\mathfrak{D}$-stability constraints, in order not only to provide recursive stability and feasibility but also to allow specifying closed-loop behavior more directly as compared to the simple manipulation of the MPC weight matrices.

The rest of this article is structured as follows: In Section 2 the model of the helicopter is presented; the main contribution, that is, the formal demonstration that the stability and recursive feasibility of the MPC scheme with move blocking is preserved with the calculation of the internal closed-loop gains through LMIs is found in Section 3, in which the adopted MPC formulation is also presented, as well as the LMI $\mathfrak{D}$-stability restrictions; simulation results comparing the solutions with internal closed-loop using a linear quadratic regulator and with the current proposal are presented in Section 4; finally, conclusions and suggestions for future work are given in Section 5.

1.1 Notations

- $\square'$ denotes the transpose of $\square$.
- $\otimes$ denotes the Kronecker product.

2. 3DOF HELICOPTER

The 3DoF helicopter is a didactic plant purposed to represent the dynamics of a real helicopter with two engines in a simplified way (Figure 1). It can perform three rotational movements: Pitch (along the body, in the plane perpendicular to the main arm), Elevation (in the plane of the main arm with the base), and Travel (in the plane perpendicular to the base). The secondary arm contains a counterweight whose purpose is to decrease the power required to maintain level flight or to impose positive Elevation accelerations.

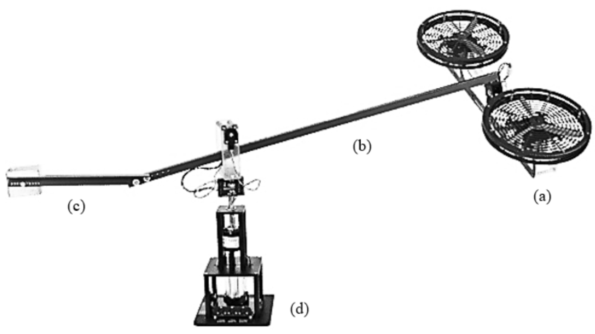

Figure 1. 3DoF helicopter – (a) body; (b) main arm; (c) secondary arm; (d) base.

The set of Ordinary Differential Equations (1) was derived from simplifications of the Lagrange Equations for modeling the 3DoF helicopter and later addition of viscous friction effect (TableA.2). This model represents the evolution of the work from Lopes (2007), Maia (2008) and Afonso et al. (2009). Tables A.1 and A.2 contain the values of linearization voltage and physical parameters of the sixth order system, respectively.

$$\dot{x_1} = x_2 \tag{1a}$$

$$\dot{x_2} = e_{16}(e_1(u_1^2 - u_2^2) + e_2(u_1 - u_2) - v_2 x_2) \tag{1b}$$

$$\dot{x_3} = x_4 \tag{1c}$$

$$\begin{aligned}\dot{x_4} = {} & x_6^2(e_3 \sin 2x_3 + e_4 \cos 2x_3) + e_5 \sin x_3 + \\ & e_6 \cos x_3 + (e_7(u_1^2 + u_2^2) + e_8(u_1 + u_2)) \cos x_1\end{aligned} \tag{1d}$$

$$\dot{x_5} = x_6 \tag{1e}$$

$$\begin{aligned}\dot{x_6} = {} & (e_{13} + e_{14} \sin 2x_3 + e_{15} \cos 2x_3)^{-1} \\ & \cdot (v_1 - v_3 x_6 + (e_9(u_1^2 + u_2^2) + e_{10}(u_1 + u_2)) \sin x_1 \\ & + x_4 x_6 (e_{11} \sin 2x_3 + e_{12} \cos 2x_3))\end{aligned} \tag{1f}$$

The matrices (2a) and (2b) represent the linearized and transformed model for the discrete-time domain with sampling period $T = 100\ ms$ and Zero-order Hold (ZOH) method (Franklin et al., 2002).

$$A = \begin{bmatrix} 1.0 & 0.0963 & 0 & 0 & 0 & 0 \\ 0 & 0.927 & 0 & 0 & 0 & 0 \\ 0 & 0 & 0.995 & 0.0998 & 0 & 0 \\ 0 & 0 & -0.104 & 0.995 & 0 & 0 \\ -0.00662 & -2.17 \times 10^{-4} & 0 & 0 & 1.0 & 0.0978 \\ -0.131 & -0.00645 & 0 & 0 & 0 & 0.957 \end{bmatrix} \tag{2a}$$

$$B = \begin{bmatrix} 0.0145 & -0.0145 \\ 0.286 & -0.286 \\ 0.00208 & 0.00208 \\ 0.0416 & 0.0416 \\ -1.62 \times 10^{-5} & 1.62 \times 10^{-5} \\ -6.44 \times 10^{-4} & 6.44 \times 10^{-4} \end{bmatrix} \tag{2b}$$

3. MPC WITH MOVE BLOCKING

The matrices in (2) compose the discrete, linear, and time-invariant equation of states

$$x(k+1) = Ax(k) + Bu(k), \tag{3}$$

where $x(k)$ is the state measured at time k. Let x_i denote the predicted state at instant $k+i$, given $x(k)$ and a control sequence $(u_0, ..., u_{i-1})$. Also, assume that the states and inputs are subject to the constraints

$$x(k) \in \mathbb{X} \subseteq \mathbb{R}^n,\ u(k) \in \mathbb{U} \subseteq \mathbb{R}^m,\ \forall k \geqslant 0, \tag{4}$$

such that $\mathbb{X}$ and $\mathbb{U}$ are compact polyhedral sets containing the origin in the interior.

The proposed control law comes from Cagienard et al. (2007):

$$V_N^*(x, T) := \min_{\hat{c}_0, \ldots, \hat{c}_{M-1}} \sum_{i=0}^{N-1} (u_i' R u_i + x_i' Q x_i) + x_N' P x_N, \tag{5a}$$

subject to:

$$x_i \in \mathbb{X},\ u_i \in \mathbb{U},\ \forall i \in \{0, ..., N-1\}, \tag{5b}$$
$$x_\ell \in \mathscr{X}(K),\ \ell = \mathrm{rows}(T), \tag{5c}$$
$$\left[c_0', ..., c_{\ell-1}'\right]' = (T \otimes I_m)\left[\hat{c}_0', ..., \hat{c}_{M-1}'\right]', \tag{5d}$$
$$c_i = 0,\ \forall i \in \{\ell, ..., N-1\}, \tag{5e}$$
$$u_i = Kx_i + c_i,\ \forall i \in \{0, ..., N-1\}, \tag{5f}$$
$$x_{i+1} = Ax_i + Bu_i,\ x_0 = x(k),\ \forall i \in \{0, ..., N-1\}, \tag{5g}$$

with the following definitions:

• P, Q and R are positive-definite and symmetric matrices. Q and R balance the input and state signals weight on the cost function, respectively. The P matrix is the solution of the algebraic Riccati equation (6), which guarantees closed-loop stabilization gains through Equation (7):

$$P = A^T PA - A^T PB\left(B^T PB + R\right)^{-1} B^T PA + Q, \tag{6}$$
$$K = -\left(B^T PB + R\right)^{-1} B^T PA. \tag{7}$$

• $\mathscr{X}(K)$ denotes the maximum positive invariant set for the linear system (3) that satisfies the restrictions in (4) through the control law $u(k) = Kx(k)$. The terminal constraint $x_\ell \in \mathscr{X}(K)$ guarantees recursive feasibility for the optimization problem for all time.

• $T \in \{0,1\}^{\ell \times M}$ stands for the current *blocking matrix*, which reduces the minimization cost (5a) through the solution of $\left[\hat{c}_0', ...\hat{c}_{M-1}'\right]' \in \mathbb{R}^{mM}$, instead of the full vector $\left[c_0', ...c_{N-1}'\right]' \in \mathbb{R}^{mN}$. Such a strategy diminishes the computational complexity of the control problem by reducing the number of optimization variables (Gondhalekar and Imura, 2010). Conventionally, one would start with $T \in \{0,1\}^{N\times N}$ and reduce the dimension of the control horizon (T columns) through $M < N$. However, we can have $M \leqslant \ell < N$ with the blocking matrix to hold several input values along the prediction horizon (T rows), not only from $M+1$ to N. $T(k+1) = f(T(k))$ is computed recursively at each iteration by Algorithm 1:

Algorithm 1 Move blocking function

if $\ell = 1$ **then**
  $f(T) \coloneqq \mathbf{1}_{N\times 1}$
else if $\ell > 1$ **then**
  $S \coloneqq \begin{bmatrix} \mathbf{0}_{(\ell-1)\times 1} & I_{\ell-1} \end{bmatrix} T$
  if $S(1,1) = 1$ **then**
    $f(T) \coloneqq S$
  else
    $W \coloneqq S \begin{bmatrix} \mathbf{0}_{1\times(M-1)} & 0 \\ I_{M-1} & \mathbf{0}_{(M-1)\times 1} \end{bmatrix}$
    $f(T) \coloneqq \begin{bmatrix} W \\ \mathbf{0}_{(N-\ell+1)\times(M-1)} \ \ \mathbf{1}_{(N-\ell+1)\times 1} \end{bmatrix}$
  end if
end if
return $f(T)$

3.1 Redesign of the internal control-loop

Cagienard et al. (2007) proves a theorem to explain how the move blocking scheme grants asymptotic stability of the closed-loop system (5g). Such a demonstration was developed considering the internal stabilizing gain array K prior computed via the algebraic Riccati equation.

In this section, we propose an adaptation to that theorem to explore the capability of Algorithm 1 with the premise to compute K using LMIs while still respecting the previous proven stability and recursive feasibility of the final control law.

Theorem 1. Consider that matrix P in (5a) satisfies the following inequality:

$$(A+BK)'P(A+BK) - P + K'RK + Q < 0. \tag{8}$$

Then applying the move blocking Algorithm 1, assuming $T(0)$ admissible, makes the origin of the closed-loop system an asymptotically stable equilibrium with a region of attraction equal to the set of initially feasible states.

Proof. The optimization problem (5) is solved at each iteration k, and an optimal control sequence is obtained as a function of the current states and blocking matrix:

$$\begin{aligned} C^*(x(k),T(k)) &\coloneqq \left[c_0^*(x(k),T(k))', ..., c_{N-1}^*(x(k),T(k))'\right]' \\ &\coloneqq (T(k)\otimes I_m)\,\widehat{C}^*(x(k),T(k)). \end{aligned}$$

A candidate solution for problem (5) at time step $k+1$ can be obtained based on

$$\begin{aligned} &\widetilde{C}(x(k+1), T(k+1)) \\ &\quad = \left[c_1^*(x(k),T(k))', ..., c_{N-1}^*(x(k),T(k))', 0\right]'. \end{aligned} \tag{9}$$

It is easy to verify that the candidate fulfills the constraints (5b)–(5g), therefore the problem is recursively feasible. For conciseness, this verification is not included in this paper.

Given that $\tilde{c}_i = c_{i+1}^*$, one can similarly write and expand the cost function (5a) of the candidate, i.e.

$$\begin{aligned} \widetilde{V}_N(x(k+1), T(k+1)) &= \sum_{i=0}^{N-1}(\tilde{u}_i'R\tilde{u}_i + \tilde{x}_i'Q\tilde{x}_i) + \tilde{x}_N'P\tilde{x}_N \\ &= \sum_{i=0}^{N-2}\left[\tilde{u}_i'R\tilde{u}_i + \tilde{x}_i'Q\tilde{x}_i\right] \\ &\quad + \left[\tilde{u}_{N-1}'R\tilde{u}_{N-1} + \tilde{x}_{N-1}'Q\tilde{x}_{N-1}\right] + \tilde{x}_N'P\tilde{x}_N \\ &= \sum_{i=1}^{N-1}\left[u_i^{*'}Ru_i^{*'} + x_i^{*'}Qx_i^{*'}\right] \\ &\quad + \left[\tilde{u}_{N-1}'R\tilde{u}_{N-1} + \tilde{x}_{N-1}'Q\tilde{x}_{N-1}\right] + \tilde{x}_N'P\tilde{x}_N \end{aligned}$$

$$\begin{aligned} =&V_N^*(x(k),T(k)) - \left[u_0^*(k)'Ru_0^*(k) + x_0^*(k)'Qx_0^*(k)\right] \\ &- x_N^{*'}Px_N^* + \left[\tilde{u}_{N-1}'R\tilde{u}_{N-1} + \tilde{x}_{N-1}'Q\tilde{x}_{N-1}\right] + \tilde{x}_N'P\tilde{x}_N. \end{aligned}$$

Moreover, we can use that $\tilde{c}_{N-1} = c_N^* = 0$ to simplify the input and state terms:

$$\begin{aligned} \tilde{u}_{N-1} &= K\tilde{x}_{N-1} + \tilde{c}_{N-1} = Kx_N^*, \\ \tilde{x}_N &= A\tilde{x}_{N-1} + B\tilde{u}_{N-1} = (A+BK)\,x_N^*. \end{aligned}$$

Finally, we get the following expression:

$$\begin{aligned} &\widetilde{V}_N(x(k+1), T(k+1)) \\ &\quad = V_N^*(x(k),T(k)) - \left[u_0^*(k)'Ru_0^*(k) + x_0^*(k)'Qx_0^*(k)\right] \\ &\quad + x_N^{*'}\left[(A+BK)'P(A+BK) - P + K'RK + Q\right]x_N^*. \end{aligned} \tag{10}$$

In view of the optimization of the cost, it follows that

$$V_N^*(x(k+1), T(k+1)) \leqslant \widetilde{V}_N(x(k+1), T(k+1)). \tag{11}$$

Subtracting $V_N^*(x(k), T(k))$ from both sides of the inequality in (11) yields

$$\begin{aligned} V_N^*(x(k+1), T(k+1)) - V_N^*(x(k), T(k)) \leqslant \\ -\left[u_0^*(k)' R u_0^*(k) + x_0^*(k)' Q x_0^*(k)\right] \\ + x_N^{*'}\left[(A+BK)' P (A+BK) - P + K' R K + Q\right] x_N^*. \end{aligned} \quad (12)$$

By design $Q, R > 0$, therefore the first term between brackets in the right-hand-side of the inequality in (12) is such that:

$$-\left[u_0^*(k)' R u_0^*(k) + x_0^*(k)' Q x_0^*(k)\right] \leqslant 0$$

On the other hand, by the assumption in (8), P is calculated such that the second term is not positive. Therefore, one concludes from (12) that

$$V_N^*(x(k+1), T(k+1)) - V_N^*(x(k), T(k)) \leqslant 0. \quad (13)$$

Thus, such discrete difference makes V_N^* a Lyapunov function. Moreover, since $x_0^*(k) = x(k)$ in (12) and since the matrices are all negative definite, (13) is null only for $x(k) = 0$ and strictly negative elsewhere, proving the asymptotic convergence to the origin. □

In the following, the inequality in (8) is rewritten as an LMI by considering a symmetric and positive definite matrix $X \in \mathbb{R}^{n\times n}$ and matrices $Y = KX$ and $P = \gamma X^{-1}$. Multiplying the inequality in (8) from the left by X' and from the right by X, and applying successive Schur complements, an equivalent condition for computing P and K to satisfy (8) is obtained as the following LMI:

$$\begin{bmatrix} X & \mathbf{0}_{n\times n} & \mathbf{0}_{n\times m} & AX+BY \\ \mathbf{0}_{n\times n} & \gamma I_{n\times n} & \mathbf{0}_{n\times m} & Q^{1/2}X \\ \mathbf{0}_{m\times n} & \mathbf{0}_{m\times n} & \gamma I_{m\times m} & R^{1/2}Y \\ XA'+Y'B' & XQ^{1/2} & Y'R^{1/2} & X \end{bmatrix} > 0. \quad (14)$$

3.2 $\mathfrak{D}$-stability

The transient response of the system may be adjusted by restricting the system closed-loop eigenvalues λ to a particular region of the complex plane. This method is a high-level alternative to balance the final performance in terms of gain and damping factors, in contrast to tuning the weights Q and R in Equation (5a). Indeed, the analytic solution of the Riccati equation is being exchanged to a LMI setup perhaps more stringent in the state-feedback gains design, but that allows closer proximity with the system behavior desired characteristics (Boyd, 1994).

Equation (15) provides a structure of LMIs for the robust design of the controller gains (Lixin Gao and Anke Xue, 2004):

$$\begin{aligned} R_{11}\otimes X + R_{12}\otimes(AX+BY) + R_{12}'\otimes(AX+BY)' + \\ R_{22}\otimes\left[(AX+BY)'P(AX+BY)\right] < 0. \end{aligned} \quad (15)$$

The following parameters configure the matrices in (15) in order to restrict the eigenvalues λ according to $\Re\{\lambda\} \geqslant x_\alpha$:

$$-R_{\alpha_{11}} = -2x_\alpha, \quad (16a)$$
$$-R_{\alpha_{12}} = 1, \quad (16b)$$
$$-R_{\alpha_{22}} = 0. \quad (16c)$$

The parameters that outline a subset inside the cone with vertex $[x_v, 0]$ in $[0.95, 0]$ and internal angle $2\gamma = 90°$ are given by Equation (17) and dictate, approximately, the minimum damping of closed-loop modes:

$$R_{v_{11}} = \begin{bmatrix} -2x_v\sin\gamma & 0 \\ 0 & -2x_v\sin\gamma \end{bmatrix}, \quad (17a)$$
$$R_{v_{12}} = \begin{bmatrix} \sin\gamma & \cos\gamma \\ -\cos\gamma & \sin\gamma \end{bmatrix}, \quad (17b)$$
$$R_{v_{12}} = \begin{bmatrix} 0 & 0 \\ 0 & 0 \end{bmatrix}. \quad (17c)$$

The restriction imposed on the eigenvalues by the intersection of the mentioned regions (gray area), in parallel with LMI (14) for calculating P, yields the distribution of the closed-loop eigenvalues of Figure 2. The gains using the algebraic Riccati Equation in (6) and the Equation (7), as well as those using the LMIs (14), (16) and (17), are presented in Tables 1 and 2, respectively.

Table 1. Gains computed by the algebraic Riccati equation.

	x_1	x_2	x_3	x_4	x_5	x_6
u_1	1.5100	0.7693	0.1296	0.9427	-0.5342	-0.8603
u_2	-1.5100	-0.7693	0.1296	0.9427	0.5342	0.8603

Table 2. Gains computed by the LMIs.

	x_1	x_2	x_3	x_4	x_5	x_6
u_1	-1.0217	-0.5442	-1.5704	-3.6466	0.1970	0.4254
u_2	1.0217	0.5442	-1.5704	-3.6466	-0.1970	-0.4254

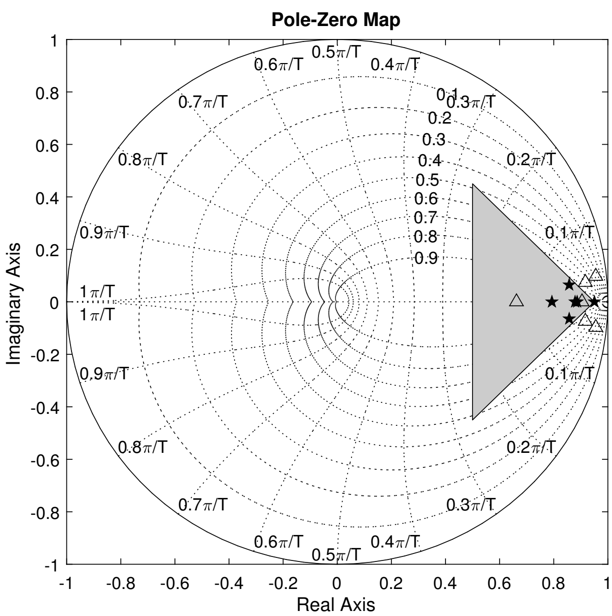

Figure 2. Closed-loop eigenvalues – (△): Riccati; (★): LMIs. The gray region displays the intersection of the areas defined by the LMIs (16) and (17).

3.3 MPC constraints definition

The quadratic optimization problem was treated by turning the cost function into a matrix format:

$$V = \mathbf{u}'\mathbf{R}\mathbf{u} + \mathbf{x}'\mathbf{Q}\mathbf{x}$$

where

$$\mathbf{u} = \begin{bmatrix} u_0 \\ u_1 \\ \vdots \\ u_{N-1} \end{bmatrix}_{mN\times 1}, \mathbf{x} = \begin{bmatrix} x_0 \\ x_1 \\ \vdots \\ x_N \end{bmatrix}_{n(N+1)\times 1},$$

$$\mathbf{R} = \begin{bmatrix} R & \mathbf{0} & \cdots & \mathbf{0} \\ \mathbf{0} & R & \cdots & \mathbf{0} \\ \vdots & \vdots & \ddots & \vdots \\ \mathbf{0} & \mathbf{0} & \cdots & R \end{bmatrix}_{mN}, \mathbf{Q} = \begin{bmatrix} Q & \mathbf{0} & \cdots & \mathbf{0} & \mathbf{0} \\ \mathbf{0} & Q & \cdots & \mathbf{0} & \mathbf{0} \\ \vdots & \vdots & \ddots & \vdots & \vdots \\ \mathbf{0} & \mathbf{0} & \cdots & Q & \mathbf{0} \\ \mathbf{0} & \mathbf{0} & \cdots & \mathbf{0} & P \end{bmatrix}_{n(N+1)}.$$

Considering the closed-loop control law $x_{i+1} = A_{cl}x_i + c_i$, with $A_{cl} = A + BK$, from (5f) and (5g), one has:

$$\mathbf{x} = \mathbf{Hc} + \mathbf{f},$$

with

$$\mathbf{H} = \begin{bmatrix} \mathbf{0} & \mathbf{0} & \mathbf{0} & \cdots & \mathbf{0} \\ B & \mathbf{0} & \mathbf{0} & \cdots & \mathbf{0} \\ A_{cl}B & B & \mathbf{0} & \cdots & \mathbf{0} \\ A_{cl}^2B & A_{cl}B & B & \cdots & \mathbf{0} \\ \vdots & \vdots & \vdots & \ddots & \vdots \\ A_{cl}^{N-1}B & A_{cl}^{N-2}B & A_{cl}^{N-3}B & \cdots & B \end{bmatrix}_{n(N+1)\times mN},$$

$$\mathbf{c} = \begin{bmatrix} c_0 \\ c_1 \\ \vdots \\ c_{N-1} \end{bmatrix}_{mN\times 1}, \mathbf{f} = \begin{bmatrix} \mathbf{I} \\ A_{cl} \\ A_{cl}^2 \\ A_{cl}^3 \\ \vdots \\ A_{cl}^N \end{bmatrix}_{n(N+1)\times n} \cdot x_0.$$

Developing the control vector, we have:

$$\mathbf{u} = \mathbf{Kx} + \mathbf{c} = (\mathbf{KH} + \mathbf{I})\,\mathbf{c} + \mathbf{Kf} = \alpha\mathbf{c} + \beta,$$

with

$$\mathbf{K} = \begin{bmatrix} K & \mathbf{0} & \cdots & \mathbf{0} & \mathbf{0} \\ \mathbf{0} & K & \cdots & \mathbf{0} & \mathbf{0} \\ \vdots & \vdots & \ddots & \vdots & \vdots \\ \mathbf{0} & \mathbf{0} & \cdots & K & \mathbf{0} \end{bmatrix}_{mN\times n(N+1)}.$$

From this, we can formulate the restrictions over the states (18) and control signals (19):

$$\begin{bmatrix} \mathbf{H} \\ -\mathbf{H} \end{bmatrix} \cdot \mathbf{c} \leqslant \begin{bmatrix} \mathbf{x_{max}}_{n(N+1)\times 1} - \mathbf{f} \\ \mathbf{f} - \mathbf{x_{min}}_{n(N+1)\times 1} \end{bmatrix}, \tag{18}$$

$$\begin{bmatrix} \alpha \\ -\alpha \end{bmatrix} \cdot \mathbf{c} \leqslant \begin{bmatrix} \mathbf{u_{max}}_{mN\times 1} - \beta \\ \beta - \mathbf{u_{min}}_{mN\times 1} \end{bmatrix}. \tag{19}$$

The simulations run in this work were configured with prediction horizon $N = 50$, control horizon $M = 20$, and $R = Q = 1$. The maximum values for each state position and velocity, respectively, were set as $\mathbf{x_{max}} = [0.2, 0.2, \infty, 0.5, \infty, \infty]'$, with $\mathbf{x_{min}} = -\mathbf{x_{max}}$. The pair $\mathbf{u_{min}} = [-2.9735, -2.9735]'$ and $\mathbf{u_{max}} = [2.0265, 2.0265]'$ constraints the excursion of the control signals around the equilibrium condition (A.1) inside the interval $[0, 5]\ V$.

4. RESULTS

The control law derived in this work was simulated in the regulation of the Elevation and Travel sates with initial conditions $-1\ rad$ and $1\ rad$, respectively. In other words, a positive initial Pitch is expected for the helicopter to climb up and move counterclockwise over the workbench. Figures 3, 4 and 5 show that the control signals, state derivatives and their trajectories, respectively, respect the limits imposed by the control law. Figure 5 depicts a more dampened response by the gains calculated via LMIs compared to the nominal gains from the algebraic Riccati equation (Figure 6) in terms of the Elevation angle.

The simulation elapsed time of the maneuver described above was approximately 22.9% shorter with the move blocking algorithm enabled, regarding the mean time value to run 500 cycles with and without using the strategy. Table 3 summarizes these results in absolute values.

Table 3. Simulation elapsed time comparison.

	Mean time $[s]$	Standard deviation $[s]$
MPC	2.84	0.153
Move blocking MPC	2.19	0.112

5. CONCLUSION

This paper verified the move blocking algorithm from Cagienard et al. (2007) as suitable for the control strategy of the 3DoF helicopter. It was formally demonstrated that the proposed method to calculate the internal-loop gains retains both stability and recursive feasibility of the MPC, and the modified set yielded an improved system response.

Future work may investigate adding robustness capabilities to handle parametric variations of the plant model and exogenous disturbance, as well as the experimental validation of this proposal. In parallel, the derived LMI setup could be used to manipulate the optimization scenario regarding the domain of attraction to grant other feasible solutions, alternative to the $\mathfrak{D}$-stability approach.

The discussed results set precedents to extend simulation of other maneuvering conditions and operation of the 3DoF helicopter aiming eventual workbench experiments. Also, a potential development would be the integration of the move blocking an MPC scheme with binary decision variables. This tool could add collision avoidance functionality to the control system.

REFERENCES

Afonso, R.J.M., Kienitz, K.H., and Galvão, R.K.H. (2009). Projeto de um controlador robusto para um modelo de um helicóptero com três graus de liberdade baseado no método LQG/LTR. In *3rd CTA-DLR Workshop on Data Analysis & Flight Control*. Instituto Tecnológico de Aeronáutica, São José dos Campos.

Boyd, S.P. (ed.) (1994). *Linear matrix inequalities in system and control theory*. Number vol. 15 in SIAM studies in applied mathematics. Society for Industrial and Applied Mathematics, Philadelphia.

Cagienard, R., Grieder, P., Kerrigan, E., and Morari, M. (2007). Move blocking strategies in receding horizon control. *Journal of Process Control*, 17(6), 563–570. doi: 10.1016/j.jprocont.2007.01.001.

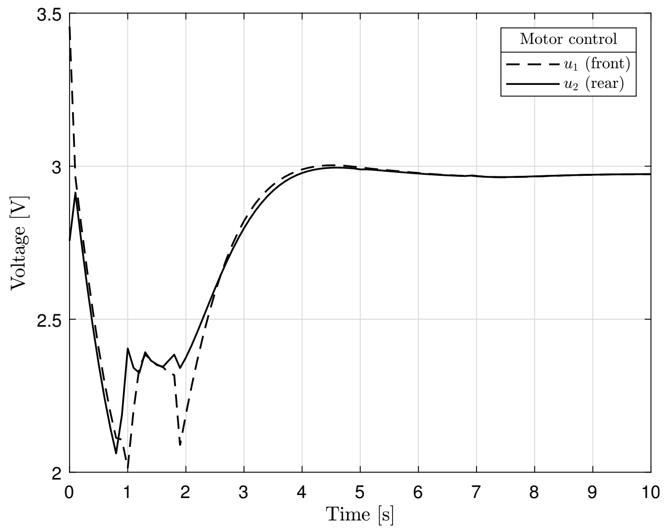

Figure 3. Control signals with the internal control-loop gains computed through LMIs.

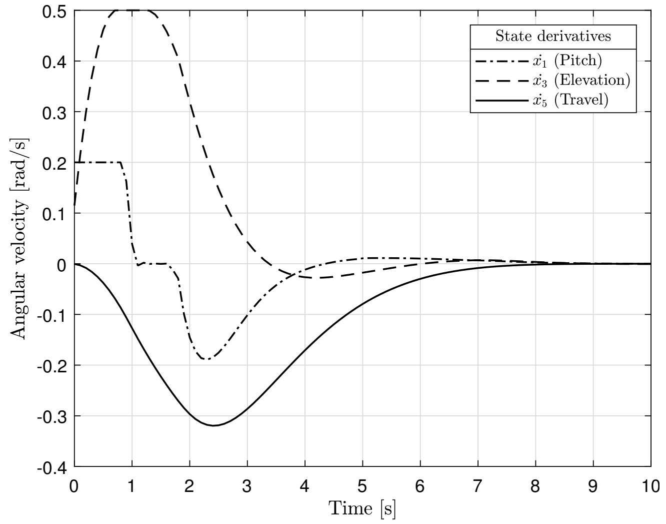

Figure 4. State derivatives response with the internal control-loop gains computed through LMIs.

Caregnato Neto, A. (2018). *Multirate Control of a 3DoF Helicopter.* Dissertation of Master of Science, 87p, Instituto Tecnológico de Aeronáutica, São José dos Campos.

Chung, R.H.H. (2017). *Controle Preditivo Robusto para Manobra com Desvio de Obstáculos de um Helicóptero com Três Graus de Liberdade.* Dissertation of Master of Science, 108p, Instituto Tecnológico de Aeronáutica, São José dos Campos.

Franklin, G.F., Powell, J.D., and Workman, M.L. (2002). *Digital control of dynamic systems.* Addison-Wesley, Menlo Park, Calif., 3. ed., [nachdr.] edition. OCLC: 249361424.

Gondhalekar, R. and Imura, J.i. (2010). Least-restrictive move-blocking model predictive control. *Automatica*, 46(7), 1234–1240. doi:10.1016/j.automatica.2010.04.010.

Lixin Gao and Anke Xue (2004). On LMI robust D-stability condition for real convex polytopic uncertainty. In *Fifth World Congress on Intelligent Control and Automation (IEEE Cat. No.04EX788)*, volume 1, 151–

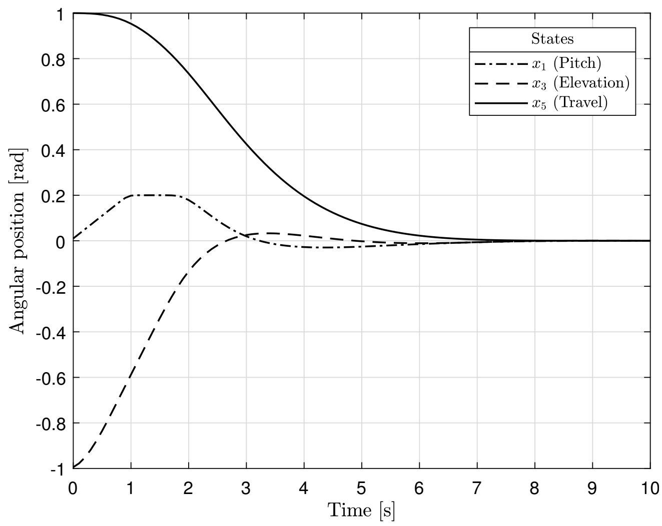

Figure 5. State excursion response with the internal control-loop gains computed through LMIs.

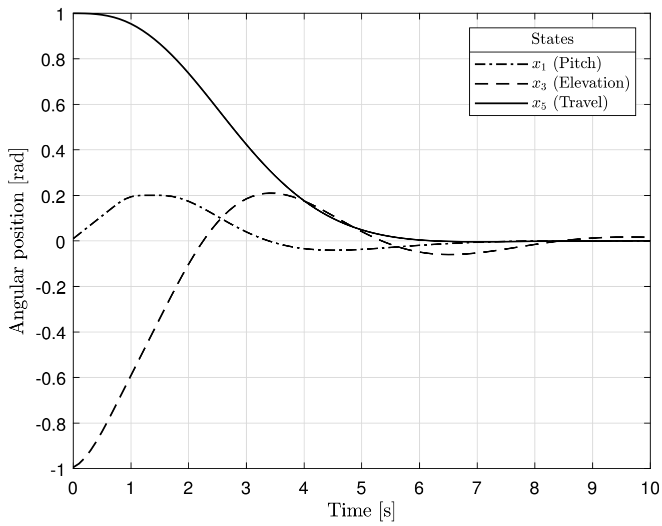

Figure 6. State excursion response with the internal closed-loop gains computed through the algebraic Riccati equation.

154 Vol.1. doi:10.1109/WCICA.2004.1340544.

Lopes, R.V. (2007). *Modelagem e Controle Preditivo de um Helicóptero com Três Graus de Liberdade.* Dissertation of Master of Science, 136p, Instituto Tecnológico de Aeronáutica, São José dos Campos.

Maciejowski, J.M. (2002). *Predictive control: with constraints.* Prentice Hall, Harlow, England ; New York.

Maia, M.H. (2008). *Controle Preditivo Robusto de um Helicóptero com Três Graus de Liberdade Sujeito a Perturbações Externas.* Dissertation of Master of Science, 117p, São José dos Campos.

Mayne, D.Q., Rawlings, J.B., Rao, C.V., and Scokaert, P.O.M. (2000). Constrained model predictive control: Stability and optimality. *Automatica*, 36(6), 789–814. doi:10.1016/S0005-1098(99)00214-9.

Pascoal, R.M. (2010). *Controle Preditivo Robusto para um Helicóptero com Três Graus de Liberdade.* Dissertation of Master of Science, 96p, Instituto Tecnológico de Aeronáutica, São José dos Campos.

Rossiter, J.A. (2003). *Model-based predictive control: a practical approach.* Control series. CRC Press, Boca Raton.

Appendix A. MODEL PARAMETERS

Table A.1. Inputs: equilibrium condition.

Motor	Voltage $[V]$
u_1	2.9735
u_2	2.9735

Table A.2. Plant parameters.

Parameter	Value
v_1	$0\ N \cdot m$
v_2	$0.18\ N \cdot s$
v_3	$0.47\ N \cdot m \cdot s$
e_1	$0.1117\ N/V^2$
e_2	$0.0449\ N/V$
e_3	-0.4843
e_4	0.1153
e_5	$-1.0389\ N/(m \cdot kg)$
e_6	$-1.3170\ N/(m \cdot kg)$
e_7	$0.0656\ N/(m \cdot kg \cdot V^2)$
e_8	$0.0264\ N/(m \cdot kg \cdot V^2)$
e_9	$-0.0718\ N \cdot m/V^2$
e_{10}	$-0.0289\ N \cdot m/V$
e_{11}	$1.0567\ kg \cdot m^2$
e_{12}	$-0.2515\ kg \cdot m^2$
e_{13}	$0.5454\ kg \cdot m^2$
e_{14}	$0.1258\ kg \cdot m^2$
e_{15}	$0.5283\ kg \cdot m^2$
e_{16}	$4.1832\ (m \cdot kg)^{-1}$